On Magnetic Fields and MHD Equilibria in Stellarators

Bernhard Seiwald

Betreuer:
Ao.Univ.-Prof. Dipl.-Ing. Dr.phil. Martin Heyn
Institut für Theoretische Physik - Computational Physics
Technische Universität Graz

19. 09. 2007

Graz University of Technology

Outline

Outline

Introduction

Several ways to achieve fusion, e.g.:

gravitational confinement Strong gravitation enables the fusion - the mechanism in stars.

inertial confinement A very dense plasma is created by compression of small pellets of Deuterium-Tritium fuel using laser driven implosion.

magnetic confinement A plasma is confined in a magnetic field for a sufficiently long time.

The work is done in the framework of international cooperations (EURATOM) to make fusion accessible as an energy source.

Toroidal Magnetic Confinement

Simple toroidal fields do not confine plasma properly, because of particle drift.

$\longrightarrow$ Helical twist of field lines is necessary for confinement.

Two ways to achieve the helical twist:

- Tokamak (rus.: “toroidal’naya kamera s magnitnymi katushkami”, engl.: “toroidal chamber with magnetic coils”): uses external driven toroidal plasma current.
- Stellarator: predominately external magnetic field coils.

Tokamak

Scheme of a Tokamak

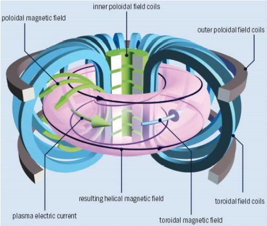

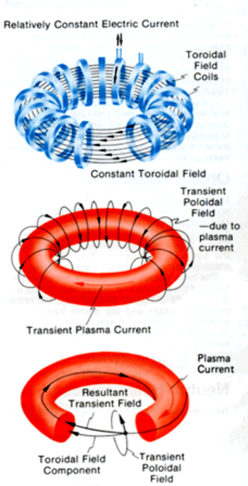

ITER

International
Thermonuclear
Experimental Reactor

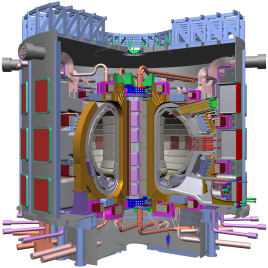

$R = 6.2$ m, $a \approx 2$ m

Schemes of Stellarators

LHD
NIFS, Toki-city, Japan

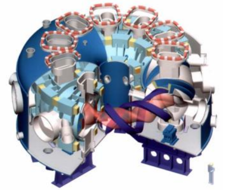

$R = 3.9$ m, $a \approx 0.65$ m

TJ-II
CIEMAT, Madrid

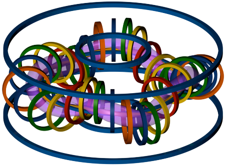

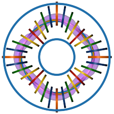

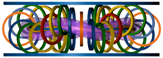

$R = 1.5$ m, $a < 0.22$ m

W7-X
Max-Planck-Institut für Plasmaphysik, Greifswald

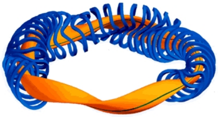

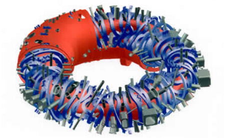

$R = 5.5$ m, $a \approx 0.53$ m

Outline

VMEC_PP - Motivation

VMEC (Variational Moments Equilibrium Code) computes magnetohydrodynamic (MHD) equilibria for nested magnetic flux surfaces. VMEC uses the energy principle to obtain the solution of the MHD equilibrium equation

$$\mathbf{J} \times \mathbf{B} - \nabla p = 0 \tag{1}$$

considering nested magnetic flux surfaces.

Problem: Singular behavior of force equation near the magnetic axis because of the used coordinate system.

VMEC_PP - Coordinate Systems

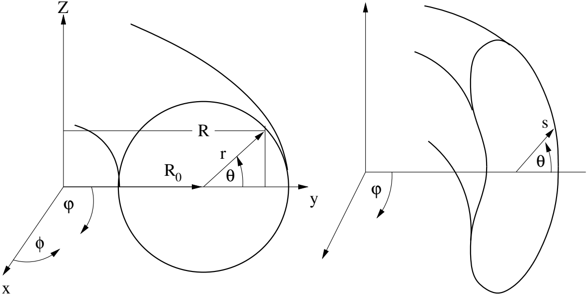

The “cylindrical-toroidal” (left) and the VMEC (right) coordinate system which are used for the calculations for the standard tokamak.

VMEC_PP - Coordinate Systems

The poloidal and the toroidal periodicity allow 2D Fourier representation.

$$R(s,\theta,\varphi) = \sum_{m=0}^{m_{\mathrm{pol}}} \sum_{n=-n_{\mathrm{tor}}}^{n_{\mathrm{tor}}} R_{mn}(s)\cos(m\theta - Nn\varphi)\,, \tag{2a}$$

$$Z(s,\theta,\varphi) = \sum_{m=0}^{m_{\mathrm{pol}}} \sum_{n=-n_{\mathrm{tor}}}^{n_{\mathrm{tor}}} Z_{mn}(s)\sin(m\theta - Nn\varphi)\,, \tag{2b}$$

$$B(s,\theta,\varphi) = \sum_{m=0}^{m_{\mathrm{pol}}} \sum_{n=-n_{\mathrm{tor}}}^{n_{\mathrm{tor}}} B_{mn}(s)\cos(m\theta - Nn\varphi)\,, \tag{2c}$$

with N the number of field periods, on a radial grid of the normalized toroidal flux (s) with $m_{\mathrm{pol}}+1$ and $2n_{\mathrm{tor}}+1$ poloidal and toroidal modes.

VMEC_PP - Properties of the Algorithm

- Regularization of the flux surface coordinates with smoothing spline.
  - Implementation of the square root characteristic for $s \longrightarrow 0$.
  - Semiautomatic control of the strength of the smoothing.
- Consistent recalculation of the magnetic field data.
  - Guarantee for a divergence free magnetic field up to computer accuracy.

$\Rightarrow$ Method has been tested on a torus with circular cross sections (named "standard tokamak"), because its equilibrium can be calculated analytically.

VMEC_PP - Application to W7-AS and Result

$|B|$ of the configuration s31114.14

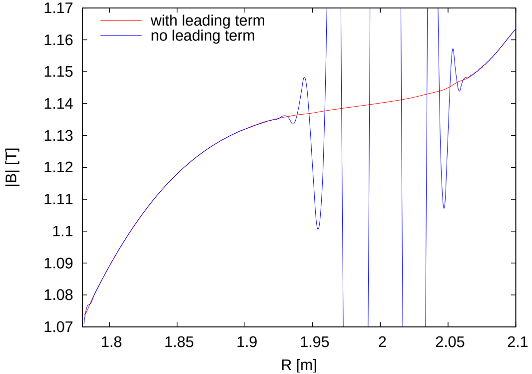

Both curves are calculated with the smoothing spline.

With and without taking into account square root characteristics.

VMEC_PP - Application to W7-AS and Result

Coefficients of the configuration s31114.14

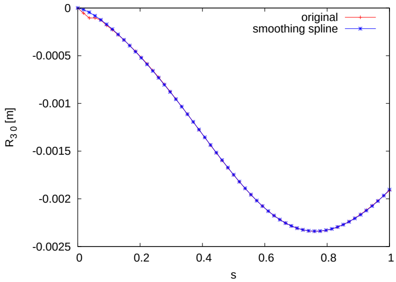

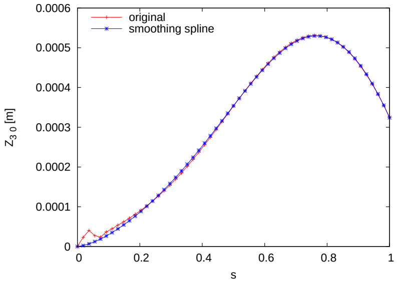

Original, calculated by VMEC; smoothed by the smoothing spline.
The smoothing procedure developed within this work acts locally without effecting the global behavior, as intended.

Outline

Stellarator Optimization

A Method for Optimizing Stellarators in Real Space Coordinates

- 3D geometry enables large number of possible variations of stellarators.
- Designing stellarators $\longrightarrow$ existing programs.
- International interest in optimizing existing stellarators.
    - Goal: maximizing the total stored energy in the plasma volume.
    - Fully realistic calculation not possible $\rightarrow$ focus on reactor relevant transport regime (long mean free path regime).

Physics

Particles may be trapped (single, multiply) or untrapped.

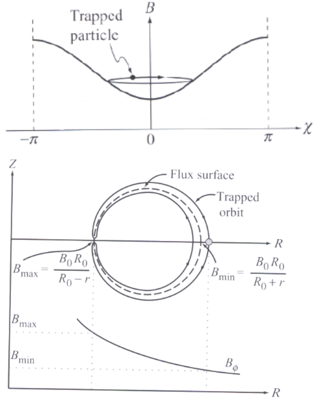

Tokamak: symmetric field, banana orbit closed.

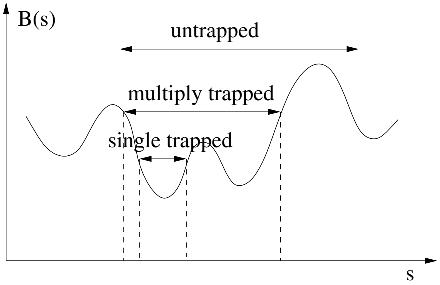

Stellarator: no symmetric field, banana orbit not closed, banana orbit drifts.

Transport Regimes

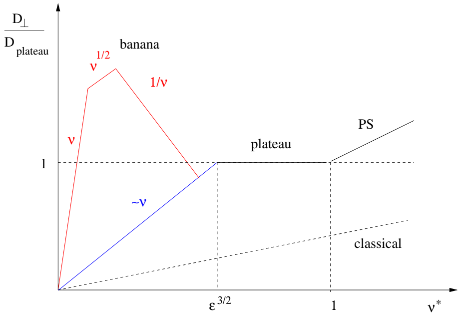

Transport coefficients as functions of the collision frequency ($\nu^* = \nu \; R \; q \; / \; v_T$, collision frequency ν, torus radius R, safety factor $q = 1/\iota$, thermal velocity v_T).

Banana regime: tokamak (ν), stellarator ($1/\nu$).

Plateau regime (independent of ν).

Pfirsch-Schlüter (PS) regime (ν).

Heat conductivity equation: $$\frac{1}{r}\frac{\partial}{\partial r} r \kappa_\perp \frac{\partial T}{\partial r} + Q(r) = 0 \tag{3}$$

Boundary conditions: $$T(a) = 0 \quad \text{and} \quad \lim_{r\to 0}\left(r\frac{\partial T}{\partial r}\right) = 0 \tag{4}$$

Diffusion coefficient: $$D_{neo} = \omega_B^2 \nu_{eff}\, n_{tr}/n \propto (1/\sqrt{\epsilon})^2\, 1/\epsilon\,\sqrt{\epsilon} \tag{5}$$

Normalized stored energy: $$\hat{W} = \int_0^a \mathrm{d}r\; r\,\hat{n}(r)\left(\int_r^a \frac{dr'}{r'\,\epsilon_{\text{eff}}^{3/2}(r')}\right)^{2/9} \tag{6}$$

Effective ripple ϵ_{eff}

$$\epsilon_{\mathrm{eff}}^{3/2} = \frac{\pi R^2}{8\sqrt{2}} \lim_{L_s\to\infty} \left(\int_0^{L_s} \frac{\mathrm{d}s}{B} \right) \left(\int_0^{L_s} \frac{\mathrm{d}s}{B} |\nabla\psi| \right)^{-2} \cdot \int_{B_{\mathrm{min}}^{(\mathrm{abs})}/B_0}^{B_{\mathrm{max}}^{(\mathrm{abs})}/B_0} \mathrm{d}b' \sum_{j=1}^{j_{\mathrm{max}}} \frac{\hat{H}_j^2}{\hat{I}_j} \tag{7}$$

with

$$\hat{H}_j = \frac{1}{b'} \int_{s_j^{(\mathrm{min})}}^{s_j^{(\mathrm{max})}} \frac{\mathrm{d}s}{B} \sqrt{b' - \frac{B}{B_0}} \left(4\frac{B_0}{B} - \frac{1}{b'} \right) |\nabla\psi| k_{\mathrm{G}} \,, \tag{8}$$

$$\hat{I}_j = \int_{s_j^{(\mathrm{min})}}^{s_j^{(\mathrm{max})}} \frac{\mathrm{d}s}{B} \sqrt{1 - \frac{B}{B_0 b'}} \,, \qquad b' = \frac{v^2}{J_\perp B_0} = \frac{v^2 B}{v_\perp^2 B_0} \,. \tag{9}$$

Numerical Realization → SORSSA

- Simulated Annealing algorithm used for the optimization process.
  - Stochastic method. Idea borrowed from thermodynamics. Models the way how liquids crystallize during annealing process.

- Choosing currents of coil groups according to Simulated Annealing algorithm.
- Computation of field lines and ϵ_{eff}.
  - Computation of ϵ_{eff} time consuming → Parallelizing.
  - Checking field line forming a flux surface or not.
- Computation of energy $\hat{W} = \int_0^a \mathrm{d}r\, r\, \hat{n}(r) \left(\int_r^a \frac{dr'}{r'\, \epsilon_{\text{eff}}^{3/2}(r')} \right)^{2/9}$.

Result: optimal currents of coil groups (coil positions, angles between coils)

SORSSA - Application

Application to three experiments: TJ-II, U-2M, CNT

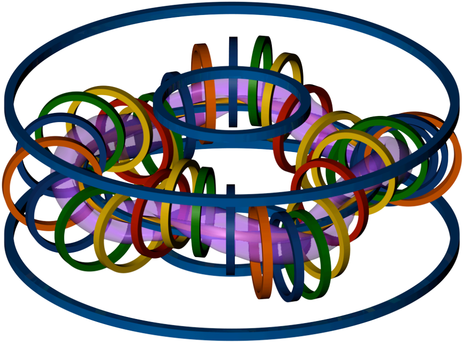

Basic parameters of TJ-II:

R=1.5 m, a<0.22 m

Coil system:

1 central circular coil,

1 central helical coil wrapped around the central circular coil,

vertical field coils,

32 toroidal coils, helically displaced.

Optimization: $I_{\mathrm{std}} \pm 20\%$

Sketch of the TJ-II coil configuration (by courtesy of V. Tribaldos). The different toroidal coil groups are in different colors.

Poincaré Plots

Poincaré plots (Cross sections) at $\varphi = 0^\circ$

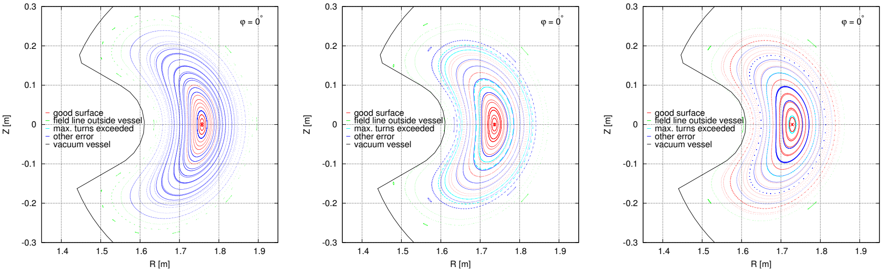

de-optimized config. standard config. optimized config.

flux surface

islands or stochastic zones

fieldline intersects vacuum vessel

Effective Ripple $\epsilon_{\text{eff}}^{3/2}$

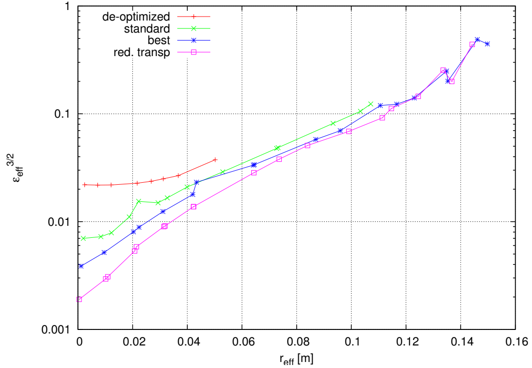

poor confinement, small volume

configuration used in experiments

optimized configuration

partly optimized: lower transport, smaller volume

$$\hat{W}_{best} \approx 1.45\ \hat{W}_{std}$$
$$\hat{W}_{red.transp.} \approx 1.42\ \hat{W}_{std}$$

Seiwald et al., International Stellarator Workshop 2005, Madrid;
Seiwald et al, J. Comput. Phys. 2007, submitted

$\theta - \varphi$ plots of $|B|$

$\theta - \varphi$ plots of $|B|$

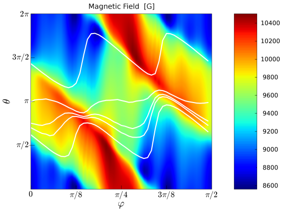

de-optimized config.

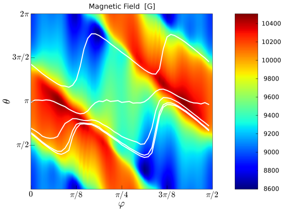

standard config.

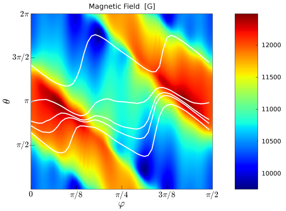

optimized config.

Summary

- SORSSA optimizes stellarators with fixed coil designs.
- The total stored energy in the plasma volume is maximized.
- Configurations with enhanced stored energy found for three experiments.
  - TJ-II presented
  - U-2M Seiwald et al., 31st EPS Conf. on Plasma Phys. London 2004; Seiwald et al., Fusion Science and Technology 2006
  - CNT Seiwald et al., 34th EPS Conf. on Plasma Phys. Warsaw 2007; Seiwald et al., Plasma Phys. Control. Fusion 2007, submitted

Thank you for your attention!

3D plots of $|B|$ for flux surfaces.

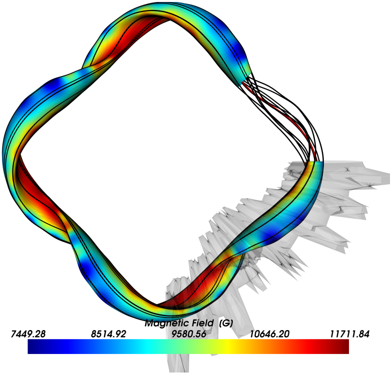

TJ-II

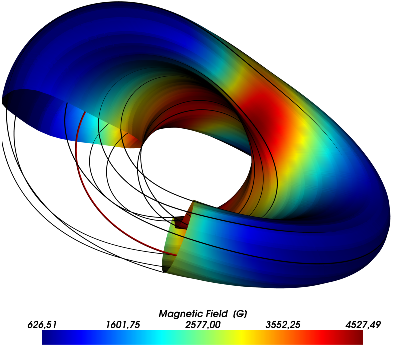

CNT

Outline

Schemes of Stellarators

CNT- Columbia Nonneutral Torus, Columbia University, NY

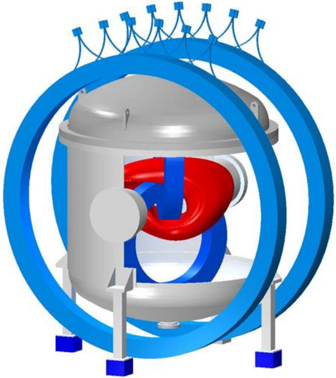

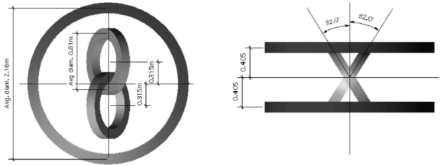

$R \approx 0.3$ m, $a \approx 0.15$ m

VMEC_PP - Algorithm 2

Smoothing spline:

$$
\begin{aligned}
S &= \frac{1}{2}\sum_{i=1}^{N}\Omega_i\left[t(s_i)\,a_i - y_i\right]^2 + \frac{1}{2}\sum_{i=1}^{N-1}\lambda_i d_i^2 \\
&+ \sum_{i=1}^{N-1}\Big[\alpha_i\left(a_i + b_i h_i + c_i h_i^2 + d_i h_i^3 - a_{i+1}\right) \\
&+ \qquad \beta_i\left(b_i + 2c_i h_i + 3d_i h_i^2 - b_{i+1}\right) \\
&+ \qquad \gamma_i\left(c_i + 3d_i h_i - c_{i+1}\right)\Big] \\
&+\chi_1\left(\mu_1 b_1 + \nu_1 c_1 + \sigma_1 b_N + \rho_1 c_N - \kappa_1\right) \\
&+\chi_2\left(\mu_2 b_1 + \nu_2 c_1 + \sigma_2 b_N + \rho_2 c_N - \kappa_2\right)\,, \qquad (10)
\end{aligned}
$$

$$
t(s) = s^{m/2}\,. \qquad (11)
$$

VMEC_PP - Algorithm 3

The choice for a semiautomatic user controlled method is:

$$\lambda_i = 1 - \Omega_i = 1 - \frac{1}{N}\sum_{i=1}^{N}\left(1 - \left(\frac{\Delta y_i}{y_{\max}}\right)^r\right). \tag{12}$$

VMEC_PP - Check a

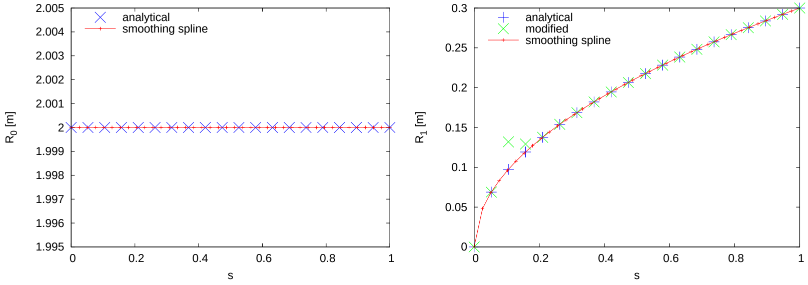

Original modes of R (blue) of the standard tokamak compared with the smoothed data from VMEC_PP (red). For the mode R_1 (lower figure) two points (green) close to the axis have been modified before smoothing.

VMEC_PP - Check b

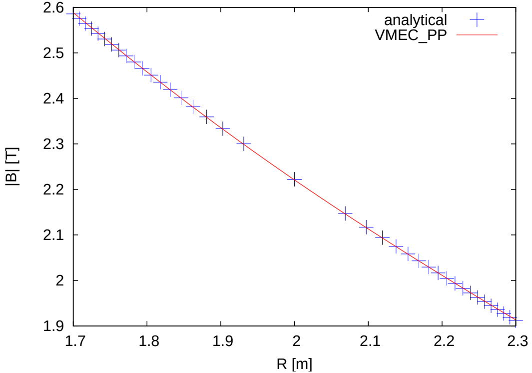

The comparison of $|\mathbf{B}|$ calculated analytically (blue) with the output of VMEC_PP (red) shows, that $|\mathbf{B}|$ is barely effected by the smoothing procedure for R_{mn} and Z_{mn}.

VMEC_PP - Application to W7-AS 3

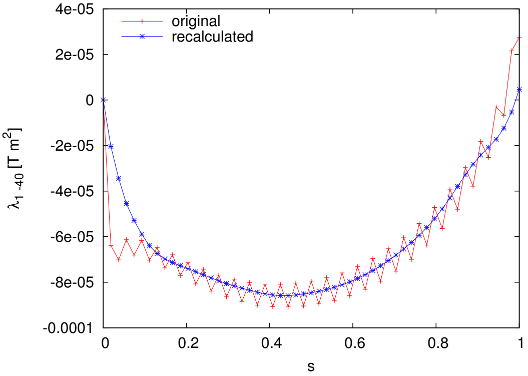

Comparison of one of the Fourier components of λ for the configuration s31114.14 calculated by VMEC (red) to the same component but consistent calculated (blue).

Variation of $|B|$

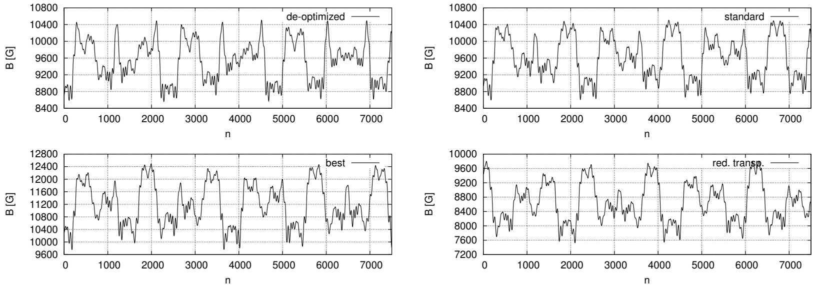

Variation of the magnetic field strength along the magnetic field line for TJ-II configurations: de-optimized, standard, best and with a markedly reduced effective ripple (n is the number of integration steps with 480 steps per magnetic field period).

Rotational Transform ι

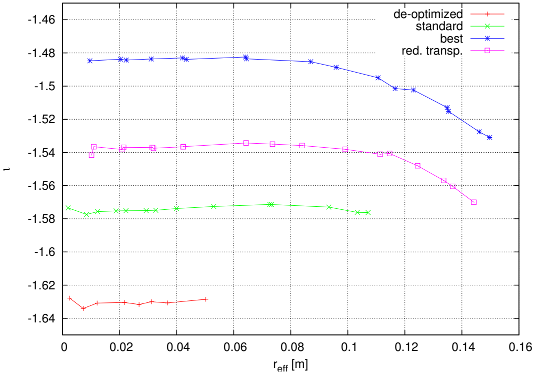

Rotational transform ι vs. effective radius r_{eff} for TJ-II configurations: de-optimized, standard, best and with a markedly reduced ("red. transp.") effective ripple.